ADAPTIVE OVERCURRENT DISTRIBUTION PROTECTION SCHEME COORDINATION IN THE PRESENCE OF DISTRIBUTED GENERATION USING ARTIFICIAL NEURAL NETWORK

TITUS OLUWASUJI AJEWOLE[1], OLUWASEYE ADETUNJI ADELEYE[*1], AMINAT OLAWUMI ABDUL-LATEEF [2]

[1]Department of Electrical and Electronic Engineering, Osun State University, Osogbo, Nigeria

[2]Department of Electrical and Electronics Engineering, Federal University of Technology, Akure, Nigeria

Received: 09 May 2023
Revised: 26 June 2023
Accepted: 20 February 2024
Published: 05 December 2024

Abstract: Recent advances in the development of distributed generation (DG) technology have resulted in increased DG penetration into distribution networks. The comparative cost advantage of its installation over grid expansion far outweighs its disadvantages. However, DG penetration introduces a lot of protection issues as a result of variation in the network short circuit current and bidirectional flow of current that, if not properly coordinated, causes maloperation of overcurrent relay protection scheme. This paper presents a novel adaptive protection scheme coordination system that uses artificial neural network (ANN) to coordinate the operations of the main and the backup relays. The proposed method determines the time settings multipliers (TMS) and the plug settings multipliers (PSM) based on the network's prevailing condition and communicates the new settings to microprocessor-based relays via optic fiber by using remote terminal unit to update the settings. The proposed scheme was applied to the IEEE 33-bus distribution network considering two different scenarios: with and without DG penetration. NEPLAN software was used to generate different fault currents required for the ANN training. Obtained simulation results show that the proposed adaptive protection scheme coordination significantly improves the protection scheme coordination with or without DG penetration.

Keywords: overcurrent relay, adaptive protection, protection coordination, distributed generation, artificial neural network

1. INTRODUCTION

Penetration of renewable energy based distributed generation (DG) into distribution networks have become one of the most researched topics nowadays. Connection of the energy sources to distribution network has many economic advantages, such as: power loss reduction, global warming reduction, enhancement of voltage profile,

* Corresponding author, email: tunjiat17@gmail.com
https://doi.org/10.29081/jesr.v30i2.001

improved power quality, higher energy operating efficiently and enhancement of network capacity [1]. Despite its huge benefits, however, penetration of DGs into distribution networks poses significant challenges to the conventional overcurrent protection scheme normally adopted for the protection of distribution networks. The conventional protection scheme is only modeled to operate for a radial distribution network with unidirectional power flow, while connection of DGs to existing networks transforms the radial distribution power flow into a meshed structure with bidirectional power. This affects the network short circuit current values of different buses [2]. The conventional overcurrent protection schemes are not designed to operate under these conditions [3]. Different DG loading equally affects the short circuit current of the network which causes the settings of the conventional relays to change regularly [4]. This causes the protection scheme of distribution networks to under/overreach during a fault, resulting in false tripping or mal-operation of the protection scheme [5]. Accurate relay coordination is required for the effective operation of the power system network. The protection system is required to isolate only the faulty section of the network while the rest sections, not affected by the fault, remain in service. This can only be achieved by effective relay coordination. Effective relay coordination is achieved by current graded systems, time graded systems or a combination of time and current graded systems. A number of studies have investigated different protection schemes deployable on distribution networks in the presence of DGs, and proposed different algorithms (linear programming and genetic algorithm) to solve the problem of loss of protection coordination between different relays connected with the network as protection scheme.

Linear programming approach to protection schemes overcurrent coordination has been versatile. Authors in [6, 7] proposed the method of disconnecting large DGs immediately after a fault current is detected; hence, avoiding the system from operating in island mode. However, these may lead to voltage sags due to the cutoff of the reactive power contribution from the DGs, thus the stability of the network is compromised if the DG penetration is high. In [8, 9], the authors proposed the method of limiting installation of DG in distribution network to maintain a constant short circuit current level. The method, however, prevents the optimal use of DGs connected to the network since increase in the penetration level of DGs is highly encouraged to reduce depletion of the ozone layer, as the method will limit penetration of the layer and thereby reduce global warming. Protection schemes by sectionalization of networks with different breakers has been proposed [10], which means reconfiguration of existing network topology. This protection scheme is costly considering the number of breakers involved and calibration of these breakers is complex as coordination of this breaker is complicated. Proposed in [11, 12] is installation of fault current limiters (FCLs) to restore relay's original settings, since FCLs have almost zero impedance in steady-state operation mode when connected to a system and introduces a high impedance in series with the system during a fault to limit its magnitude to its previous value before the installation of the DG. However, the issue of technology cost and the exact location of FCL is a major drawback. Authors in [13] proposed an adaptive protection scheme that readjusts its relay setting online to be tuned for different network operating conditions due to dispatch, but the security of the internet network may not be guaranteed. An adaptive overcurrent coordination scheme that uses differential evolution algorithm to improve the sensitivity of the backup relays as network status data obtained from the field instruments via SCADA is used to recalibrate the pickup current of different relays within the network was proposed in [14], but the method of data communication was not specified since the reliability of a system to large extent depends on the speed of the communication facility. Meanwhile, authors in [15] presented an improved adaptive protection scheme in the presence of DG by using different communication procedures. A decentralized communication system controls relays within the feeder and the centralized system controls all relays in the network. Use of a genetic algorithm (GA) to optimize time multiplier setting (TMS), as the relay time of operation depends on TMS, was proposed in [16]; while [17] proposed an approach that combines GA and dual simplex methods to calculate TMS. While in [18] the authors proposed the use of fuzzy-based GA to determine TMS, [19] proposed an adaptive protection scheme that uses both centralized and decentralized system, in which the centralized system uses microgrid central controller to change the active relay group settings by trip signal/breaker status it received from another relay or breaker. [20] presents an adaptive protection coordination scheme of DG network using a Kohonen map or selforganization map (SOM) clustering algorithm while in [21] the authors used tele protection and fuzzy system algorithm to achieve an adaptive protection system for the distribution network. While [22] submits that protection scheme can also be achieved using current and voltage extracted from the fault current, with the fault index (FI) formulated by multiplying voltage-based alienation index and current-based Wigner index used to discriminate line-to-line and double line-to-ground faults respectively; [23] proposed an adaptive protection scheme using a phasor measurement unit to mitigate the coordination challenges caused by DG placement and loading. Presented in [24] is an adaptive protection scheme coordination by using three different agents: relay agents, DG agents and equipment agents (field instruments and breakers); in which the relay agents communicate with the other two other agents for effective coordination of the protection scheme. high-speed communication equipment is, however, required in this approach to achieve reliable protection. Two different protection settings (main and backup) are proposed by

[25] for each relay, to accommodate changes as a result of DG penetration; with the main settings achieved using the positive sequence current, while the backup settings are implemented using the negative sequence.

However, the settings are complex because of extracting the positive and negative sequence currents. [26] proposed an adaptive protection scheme that calibrated and recalibrated the protection scheme based on signals released through any connecting or disconnecting of DGs in the network. However, this method is a complex and time-consuming process because if a new fault occurs while the system is attempting to determine the protection coordination settings, the system becomes vulnerable. In [27], the authors proposed an offline adaptive protection where the operational modes (grid-connected and Island) of the network are considered and settings are done in the database.

Metaheuristic approach to protection schemes overcurrent coordination has also been investigated. While in [28] the pickup current and time setting multiplier are optimized using a genetic algorithm for the DG peak and off-peak loading conditions; authors in [29] presented a method that hybridized linear programming and genetic algorithm to solve the overcurrent relay coordination problem, with genetic algorithm used to determine the pickup current setting and linear programming determined the TMS. [30] presented an adaptive protection scheme using ant colony (AC) optimization to calculate overcurrent relay time setting multipliers, while [31, 32] presented an adaptive protection scheme using a differential evolution (DE) algorithm. Despite the effectiveness of metaheuristic programming in overcurrent coordination, these studies presented overcurrent relay coordination considering only the grid-connected mode; while islanding mode and changing DG capacities, which are part of the entire system, were not considered.

Against this background, it is important to develop a hybrid adaptive overcurrent protection scheme that will respond to the prevailing distribution network conditions which are connection and disconnection of DGs connected to the network, which often time, lead to overcurrent relay coordination problems. Thus, an artificial neural network (ANN)-based adaptive over-current relay (AOR) protection scheme is proposed in this paper. The study hybridizes AOR and ANN.

The adaptive protection scheme is selected because the relays of conventional protection require recalibration each time a DG is connected into the distribution network and may likely mal-function when there is variation of short circuit current as a result of DG penetration variation. Based on this, an adaptive protection scheme that varies based on prevailing condition of the network is required and not the conventional whose setting is based on the worst case scenario. The proposed protection scheme utilizes the real-time short circuit current and voltages measured by instrument transformers located at the remote end and communicated to the local station using a remote terminal unit (RTU) via fibre optic to adjust the overcurrent time setting multiplier to be in tune with the distribution network prevailing conditions.

2. MATERIALS AND METHOD

AOR protection coordination is a protection philosophy that permits and seeks to adjust protection relay settings to make them attuned to the prevailing system conditions. This type of protection scheme is a feedback system and requires a communication link between the remote substation and the local substation [33]. ANN is a system that can modify its internal structure in relation to a function objective and so suited for solving non-linear problems being able to reconstruct the fuzzy rules that govern the optimal solution for such problems [34].

In this study, The IEEE 33-bus distribution network was modeled in NEPLAN and MATLAB software to show the efficiency of the hybrid protection scheme. The NEPLAN model was used to generate all the required short circuit current of the distribution network with and without the DG penetration. The results which were transferred to the MATLAB environment for the development of the ANN programming, which included the training of the ANN. The instrument transformer connected to the distribution substation measures the values of current and voltage and transmits the measured values to the local station via RTU connected to the circuit breakers. The data is transmitted via the power line where wave-trap and capacitor voltage transformers are used to separate the communication signal from the power signal. The transmitted data is processed by the ANN relay, and new relay settings are generated and communicated back to all the relays at the remote ends in the distribution network via the same data transmission path. The short circuit current generated was used for the setting of conventional overcurrent relay protection scheme ordination, while PSM and TSM were calculated using the short circuit current.

2.1. Conventional overcurrent relay coordination

This paper uses the inverse definite minimum time (IDMT) characteristics relay for the coordination. The operation time relay can be determined using the procedure of equations (1) to (4) [35]. Equation (1) determines the relay current I_R.

$$I_R = \frac{I_f}{I_{CT}} \tag{1}$$

where I_f is the expected fault current, while I_{CT} is the current transformer ratio. The relay pickup current I_P is obtained from:

$$I_P = P_{\text{setting}}\, xI_{SCT} \tag{2}$$

where P_{setting} is plug setting, while I_{SCT} is rated secondary current of the current transformer (CT). The plug setting multiplier (PSM) is given as:

$$PMS = \frac{I_R}{I_P} \tag{3}$$

Equation (4) gives the relay operating time.

$$T = TMS\left[\frac{A}{PMS^{\infty} + B}\right] \tag{4}$$

where A is constant (0.14,13.5 or 80) and B is a constant (-1), while ∞ is a constant that varies from 0.02 to 2. TMS varies from 0.1 to 1 at an incremental step of 0.1. In this study, the values of A, B and ∞ were taken to be 0.14, 1 and 0.02 respectively.

2.2. Power system distribution network model

Figure 1 present the distribution network, which was modeled using NEPLAN software with the parameters adapted from [36].

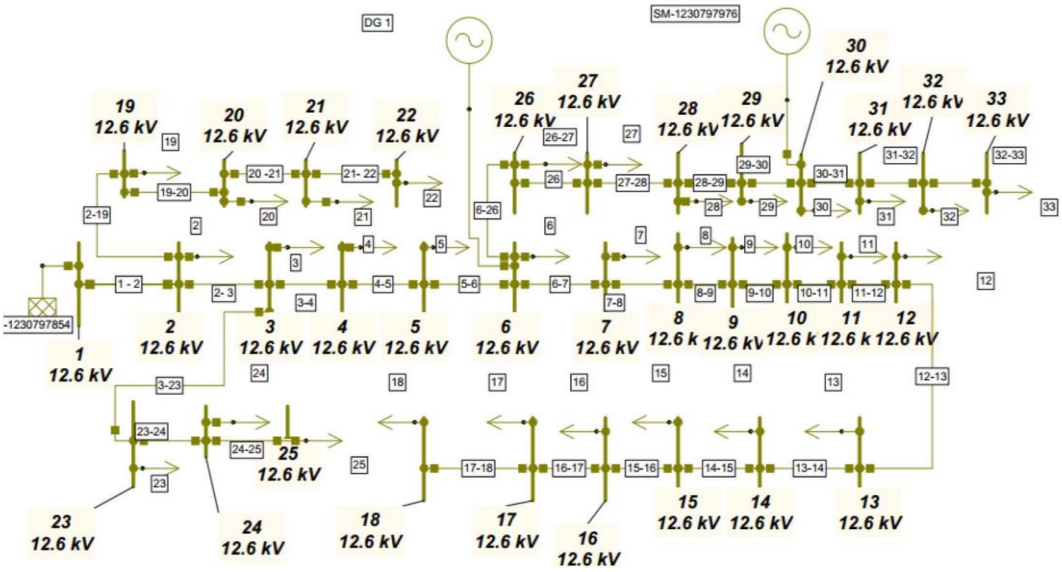

Fig. 1. IEEE 33-bus distribution network.

The network was divided into six different feeders for effective overcurrent relay coordination. The relay coordination of each feeder is independent of the protection system provided for all the feeders. Feeder 1 covers bus 1 to 5, Feeder 2 covers buses 6 to bus 12, while Feeder 3 covers buses 13-18. Feeder 4 covers buses 26-33, while Feeder 5 covers buses 19-22 and Feeder 6 covers buses 23-25. The rating of the CT used for all the protection relays varies from one feeder to another based on the load, while the voltage transformer (VT) is 12660/110V.

2.3. Adaptive overcurrent relay protection coordination

Three-phase short circuit was simulated on the IEEE 33-bus with and without DG penetration into the network to generate the required training and testing data for the artificial neural network ANN relay model. To reduce losses and achieve the desired goal of DG penetration, the optimum location and sizing techniques for DG connection that are presented in [36-38] were adopted in this study. The generated data was divided into 70% training data and 30% testing data for the ANN relay model, using Levenberg-Marquardt feed-forward/back-propagation method [39, 40]. To increase the accuracy of the ANN results and reduce the ambiguity caused by large amounts of training data, a modular ANN relay approach was adopted. The ANN mode was divided into four different models for each of the six feeders as presented in Figure 2. The proposed protection relay coordination was divided into two stages. Stage-1 presents protection relay coordination without DG, while Stage-2 presents protection relay coordination with DG. Each feeder is represented by a MATLAB code as presented in Table 1. The feeder where the fault occurred was identified with the MATLAB codes presented in Table 1 and Figure 3. This is to prevent communication breakdowns between different feeders. The control was designed with AND and OR gates which were connected at different remote buses and equally communicated with the RTU connected at local situation via fibre optic where the communicated information was processed and the time setting multiplier was sent to the ANN microprocessor-based overcurrent relay for proper relay coordination of the network.

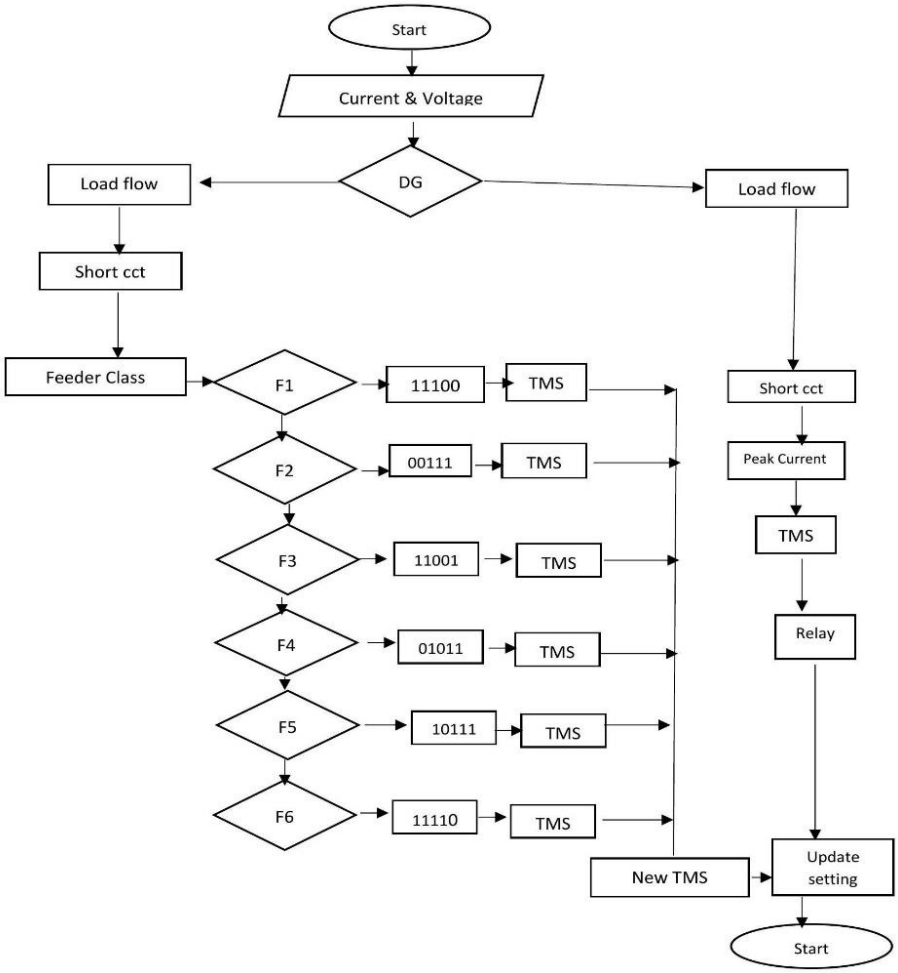

Fig. 2. Flowchart for the adaptive overcurrent protection scheme.

Table 1. MATLAB feeder code.

Feeder	Code
1	11100
2	00111
3	11001
4	01011
5	10111
6	11110

In modelling the IEEE 33-bus distribution system, a source grid rated voltage of 12.66kV/10MVAsc and reactance-to-resistance *(X/R)* ratio of 15 were used. Load flow analysis was carried out to obtain the base case result of a total real power loss of 211 kW and reactive power loss of 143kvar. The result obtained was validated as presented in [41] contains an instrument transformer with CT ratio.

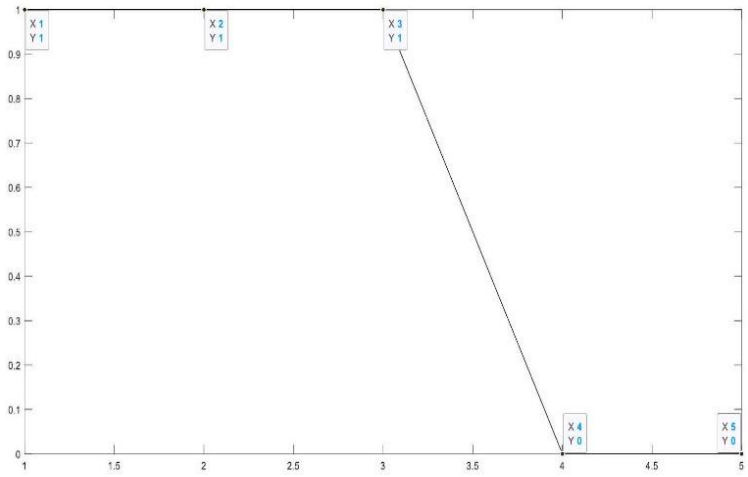

Fig. 3. Feeder identification output MATLAB code.

3. RESULTS AND DISCUSSION

Each feeder of the test distribution network (IEEE 33-Bus system) contained an instrument transformer with the current transformer (CT) ratio determined by the load current connected to that feeder. Two different cases: with and without DG penetration; were experimented on the system. Four types of short circuiting: line-to-ground (LG); three line (LLL); double-line-to-ground (LLG) and line-to-line (LL); were carried out on the distribution network, without DG penetration and with DG penetration at buses 30 and 6. However, only the LLL is reported because despite its rare frequent in occurrence, it is the most severe when it occurs.

3.1. Case I: Simulation analysis of IEEE 33-bus test system without DG penetration

Figure 4 emphasizes the fault current analysis of the short circuit experimentation carried out on the IEEE 33-bus system without DG connection. Tables 2 to 7 present the relay operations for the conventional overcurrent relay coordination of the test system.

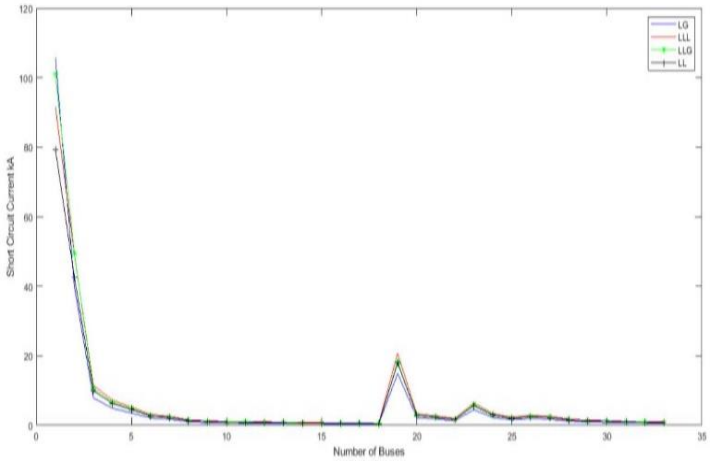

Fig. 4. Short circuit current.

Table 2 presents the relay coordination on Feeder 1. There were five relays (R1, R2, R3, R4 and R5) on the feeder. With the fault experimented at bus 6, it is noteworthy that Bus 1 and Bus 2 (to which relays R1 and R2 were connected, respectively) experienced high fault currents 91.643 A and 49.117 A, respectively. Meanwhile, the relay at the far end (that is, R5) operated first at 2.16 s with PSM/TMS of 3.462/0.6466. This was followed by R4 at 2.18 s; then R3, R2 and R1 at 2.20 s, 2.40 s and 2.60 s, respectively. With this coordination, Feeder 1 did not mal-operate.

Table 2. Overcurrent relay coordination on Feeder 1 without DG.

Relay	Fault current (kA)	PSM	TSM	Operation time (s)	Feeder operation
R1	91.643	4.675	0.9696	2.60	1
R2	49.117	3.375	0.7037	2.40	1
R3	11.42	1.486	0.2086	2.20	1
R4	7.21	4.743	0.3614	2.18	1
R5	5.207	3.462	0.6466	2.16	1

Table 3 displays the relay coordination for Feeder 2, that had a CT ratio of 800/5 A and had been controlled by seven different relays: R6, R7, R8, R9, R10, R11 and R12. With the introduction of fault at bus 13, the fairest relay (R12) operated at 0.86 s with PMS/TMS of 5.668/0.36133. This was followed by R11 at 0.96 s; R10 at 1.06 s; then R9, R8, R7 and R6 at 2.06 s, 2.08 s, 2.10 s and 2.140 s, respectively. This shows that the specified operating sequence of the feeder was followed without any mal-operation.

Table 3. Overcurrent relay coordination on Feeder 2 without DG.

Relay	Fault current (kA)	PSM	TMS	Operation time (s)	Feeder operation
R12	0.958	5.664	0.36133	0.86	2
R11	1.003	5.659	0.40313	0.96	2
R10	1.028	5.578	0.44137	1.06	2
R9	1.23	6.061	0.89995	2.06	2
R8	1.527	6.945	0.97867	2.08	2
R7	2.55	2.760	0.51288	2.10	2
R6	3.069	3.491	0.52265	2.140	2

On Feeder 3, the fault was introduced at bus 19. The relay coordination of the feeder, which had CT ratio of 800/5A, is presented in Table 4. The feeder contains six relays (R13, R14, R15, R16, R17 and R18) with relay R18 at the farmost end. When a fault occurred at bus 19 of the feeder, relay R18 operated first at 0.26 s with PMS/TMS of 2.530/0.058. This was followed by R17 that operated at 0.36 s, R16 with operating time of 0.46 s, R15 at 0.56 s, R14 at 0.66 s and R13 with operating time of 0.76 s. The feeder's relay operational coordination was highly effective and the coordination sequence was followed without any penetration from another energy source.

Table 4. Overcurrent relay coordination on Feeder 3 without DG.

Relay	Fault current (kA)	PSM	TMS	Operation time (s)	Feeder operation
R13	0.783	2.61	0.175	0.76	3
R14	0.722	2.58	0.150	0.66	3
R15	0.674	2.59	0.128	0.56	3
R16	0.625	2.60	0.106	0.46	3
R17	0.538	2.45	0.077	0.36	3
R18	0.506	2.530	0.058	0.26	3

Presented in Table 5 is the overcurrent relay coordination on Feeder 4 that had 800/5 A CT ratio. Six different relays were connected to the feeder. Fault was introduced at bus 33, and it was found that relay R33 had the least operational time of 0.80 s with PSM/TMS of 4.644/0.297. This was followed by R32 with operating time 1.00 s, R31 that operated at time 1.20 s, and R30, R29, R28, R27, R26 at 1.40 s, 1.60 s, 1.80 s, 2.0 s, 2.20 s, respectively. This shows that the calibrated sequence of operation was followed.

Table 5. Overcurrent relay coordination on Feeder 4 without DG.

Relay	Fault current (kA)	PSM	TMS	Operation time (s)	Feeder operation
R26	2.824	2.076	0.385	2.20	4
R27	2.54	1.984	0.328	2.00	4
R28	1.758	5.860	0.771	1.80	4
R29	1.425	5.089	0.630	1.60	4
R30	1.296	4.984	0.544	1.40	4
R31	1.062	4.425	0.431	1.20	4
R32	1.00	4.545	0.366	1.00	4
R33	0.931	4.655	0.297	0.80	4

The relay overcurrent protection scheme of Feeder 5 is presented in Table 6. The feeder contains four relays (R19, R20, R21 and R22). The CT connected to this feeder has 400/5 A ratio, while the fault current was introduced at bus 22. Relay R22 operated at 1.30 s with PSM/TMS of 9.520/0.71. The relay connected to bus 19, (that is, R19) was the last to energize, with operating time of 2.20 s.

Table 6. Overcurrent relay coordination on feeder 5 without DG.

Relay	Fault current (kA)	PSM	TSM	Operation time (s)	Feeder operation
R19	20.647	4.9632	0.852	2.20	5
R20	3.32	3.4583	0.568	1.90	5
R21	2.635	11.97	0.96	1.60	5
R22	1.904	9.520	0.71	1.30	5

Feeder 6 has three relays connected to it, with the CT rating of 400/5 A. Table 7 presents the sequence of operation of the feeder relays. The relay R25, which was connected to bus 25 that was the faulted bus, had the least operational time of 2.40 s with PMS/TSM of 2.8362/0.601. This was followed by R24 at 2.60 s and then R23 at 2.80 s.

Table 7. Overcurrent relay coordination of Feeder 6 without DG.

Relay	Fault current (kA)	PSM	TSM	Operation time (s)	Feeder operation
R23	6.416	1.6708	0.343	2.80	6
R24	3.349	2.4468	0.558	2.60	6
R25	2.269	2.8362	0.601	2.40	6

3.2. Case II: Simulation analysis of IEEE 33-bus system with DG penetration

With DG connected to the test system at two different connection points (buses 30 and 6), the effect of the DG penetration on the overcurrent relay coordination was studied. It must be that under this investigation, the feeders

retained their structures and attributes as in Case I. The faulted buses were also as in the previous case. Experimentation results presented in Tables 8 to 13 show the relay coordination on the feeders.

Table 8 shows the coordination on Feeder 1. The table reveals high fault current of 92.896 A and 50.624 A on buses B1 and B2, respectively. R5 operated at 2.16 s with of PSM/TSM of 4.535/0.789, after which R4 operated at 2.18 s, while R3, R2 and R1 operated at 2.20 s, 2.40 s and 2.60 s, respectively. With this coordination, Feeder 1 followed the sequence of operation obtained in Case I, but with adjustments in the TMS of the relays.

Table 8. Overcurrent relay coordination on Feeder 1 with DG.

Relay	Fault current (kA)	PSM	TSM	Operation time (s)	Feeder operation
R1	92.896	4.739	0.978	2.60	1
R2	50.624	4.349	0.852	2.40	1
R3	12.904	4.200	0.762	2.20	1
R4	8.749	23.02	0.739	2.18	1
R5	6.822	4.535	0.789	2.16	1

For Feeder 2, Table 9 presents the relay coordination. R12 operating at 0.860 seconds with PSM/TMS of 5.66/0.361 and followed by R11 at 0.96 s, R10 at 1.06 s, then R9, R8, R7 and R6 operated at 2.06 s, 2.08 s, 2.10 s and 2.14 s, respectively. It is noted from the table that the specified operating sequence of feeder was not followed.

As regards Feeder 3 shown in Table 10, R18 operated at 0.26 seconds with a PMS/TMS of 3.815/0.084. This was followed by R17 at 0.36 s, then R16 at 0.46 s, R15 at 0.56 s, R14 at 0.66 s and R13 at 0.76 s. The feeder relay operational coordination sequence was maintained, but with adjustments in the TMS.

Table 9. Overcurrent relay coordination on Feeder 2 with DG.

Relay	Fault current (kA)	PSM	TMS	Operation time (s)	Feeder operation
R6	5.168	3.49	0.522	2.14	2
R7	3.975	2.76	0.512	2.10	2
R8	2.431	6.95	0.979	2.08	2
R9	2.061	6.06	0.900	2.06	2
R10	1.841	5.58	0.441	1.06	2
R11	1.811	5.66	0.403	0.96	2
R12	1.756	5.66	0.361	0.86	2

Table 10. Overcurrent relay coordination on Feeder 3 with DG.

Relay	Fault current (kA)	PSM	TMS	Operation time (s)	Feeder operation
R13	1.614	5.380	0.309	0.76	3
R14	1.370	4.892	0.253	0.66	3
R15	1.215	4.673	0.208	0.56	3
R16	1.075	4.479	0.166	0.46	3
R17	0.834	3.790	0.115	0.36	3
R18	0.763	3.815	0.084	0.26	3

Table 11 indicates that in the Feeder 4, relay R33 had the least operational time of 0.80 s with PMS/TMS of 6.89/0.374. It was followed by R32 with operating time of 1.0 s, while R31, R30, R29, R28, R27 and R26 operated at 1.20 s, 1.40 s, 1.60 s, 1.80 s, 2.0 s and 2.20 s, respectively. This demonstrates that calibrated sequence was followed when there was DG penetration due to an adjustment in the value of TMS.

Table 11. Overcurrent relay coordination on Feeder 4 with DG.

Relay	Fault current (kA)	PSM	TMS	Operation time (s)	Feeder operation
R26	4.701	3.456	0.657	2.20	4
R27	4.184	3.268	0.570	2.00	4

R28	2.956	2.463	0.389	1.80	4
R29	2.544	9.0857	0.859	1.60	4
R30	2.376	9.1384	0.754	1.40	4
R31	1.701	7.0875	0.570	1.20	4
R32	1.545	7.0227	0.473	1.00	4
R33	1.378	6.8900	0.374	0.80	4

Table 12 presents Feeder 5 wherein R22 operated at 1.30 s with PSM/TMS of 9.530/0.714. Relay R19 was the last to operate in the feeder, with 2.20 s operating time. The sequence of operation was followed with the adjustment of TMS.

Table 12. Overcurrent relay coordination on Feeder 5 with DG.

Relay	Fault current (kA)	PSM	TSM	Operation time (s)	Feeder operation
R19	20.908	5.025	0.859	2.20	5
R20	3.327	4.620	0.703	1.90	5
R21	2.639	11.996	0.970	1.60	5
R22	1.906	9.530	0.714	1.30	5

The relay sequence of operation presented in Table 13 shows that on Feeder 6, the relay connected to bus 25 (that is, R25) had the least operational time, 2.40 s, with PSM/TMS of 3.092/0.865. With 2.80 s, relay R23 had the highest operation time.

Table 13. Overcurrent relay coordination of feeder 6 settings with DG.

Relay	Fault current (kA)	PSM	TSM	Operation time (s)	Feeder operation
R23	6.861	1.79	0.486	2.80	6
R24	3.464	2.56	0.786	2.60	6
R25	2.321	3.092	0.865	2.40	6

3.3. Comparing the operations of the distribution network with and without DG penetration

Contained in Tables 2 to 7 are the simulated fault currents at different buses, PSM, TSM and the actual relay operation times when DG has not been connected to the test system. Comparative analysis of the tables shows that the major parameter that determines the actual time of operation of the relays is the TMS. Tables 8 to 13 contain the simulated fault currents at different buses, PSM, TSM and the actual relay operation times when DG was connected to the test system. Comparative analysis of these tables reveals that the sequence of operation obtained in case I, was followed during Case II investigations only with the adjustment of the TMS of the different relays.

A comparison between Tables 2 and 8 for Feeder 1 shows that the penetration of DG increases the short circuit which is the major parameter considered during the calibration of the feeder relay. The increase in fault current has resulted into an increase in PSM and TSM which affected the relay operational parameters. Further comparisons between Tables 3 and 9, Tables 4 and 10, Tables 5 and 11, and Tables 6 and 12 show that the TMS and PSM vary as the fault current changed due to DG penetration.

Therefore, there is a need for an adaptive overcurrent protection scheme relay coordination that automatically adjusts the settings based on the current power system condition rather than on the worst-case scenario.

3.4. Adaptive overcurrent protection scheme

To normalize the output of the ANN overcurrent relay model, the output values of the ANN trip signal 1 and 0, was set at 0.7 threshold, which means above 0.7 were treated as 1 and below were treated as 0. Figure 4 represents input data of the ANN relay model simulation with and without DG. The ANN was configured with the parameters presented in Table 1. Due to the difficulty in determining the network architecture and size, the training was done by arbitrarily selecting network architecture (number of hidden layers). Several training architectures were used during the training stages, but Table 14 presents only the training architecture that satisfied the set goal (minimum square error) for the different feeders. The RTU connected to the different buses monitored the connection and disconnection of the DGs. The SCADA system processed the information and communicated the new relay setting

to the microprocessor-based overcurrent relay that in turn updated the relay setting. The percentage error in the output of the ANN overcurrent relay model was obtained from [39] as:

$$\%\ Error = \frac{ANN\ Output - Desired\ Output}{Desired\ Output} \times \frac{100}{1} \quad (5)$$

Tables 15 to 26 present the new feeder relay setting with and without DG penetration. The percentage error is presented in each. The comparison of the results shows that the ANN model constantly adjust the TMS of the relay to the achieved constant relay operational time as observed from the tables.

Table 14. ANN simulation for overcurrent relay model.

No of hidden layer	Feeder 1 (30 20 10 5)	Feeder 2 (35 25 20 15)	Feeder 3 (10 8 5 3)	Feeder 4 (40 30 25)	Feeder 5 (40 36 8 5)	Feeder 6 (30 20 10 5)
MSE achieved	0.000456	0.00088	0.00005	0.00003	0.000025	0.000109
Epoch	398	112	65	342	188	238
r_T	0.99996	0.996	0.9965	0.99987	0.99967	0.99976
r_v	0.99995	0.9965	0.9967	0.99867	0.999675	0.99786
r_{test}	0.999985	0.9945	0.99545	0.99965	0.99643	0.99967
r_{all}	0.9999965	0.9976	0.99907	0.99785	0.99965	0.99976

Table 15. Relay simulation model Feeder 1 without DG.

Relay	Fault current without DG (kA)	Desired PSM	ANN PSM	% difference PSM	Desired TMS	ANN TMS	% difference TMS	Time of operation
R1	91.643	4.675	4.768	0.019	0.9696	0.9788	0.0095	2.60
R2	49.117	3.375	3.478	0.0305	0.7037	0.7089	0.0074	2.40
R3	11.42	1.486	1.587	0.068	0.2086	0.2676	0.282	2.20
R4	7.21	4.743	4.878	0.028	0.3614	0.378	0.046	2.18
R5	5.207	3.462	3.56	0.028	0.6466	0.6687	0.034	2.16

Table 16. Relay simulation model Feeder 1 with DG.

Relay	Fault current with DG (kA)	Desired PSM	ANN PSM	% difference PSM	Desired TMS	ANN TMS	% difference PSM	Time of operation
R1	92.896	4.739	4.898	0.034	0.978	0.988	0.010	2.60
R2	50.624	4.349	4.398	0.011	0.852	0.864	0.014	2.40
R3	12.904	4.200	4.256	0.013	0.762	0.767	0.006	2.20
R4	8.749	23.02	23.09	0.003	0.739	0.745	0.008	2.18
R5	6.822	4.535	4.675	0.031	0.789	0.790	0.0013	2.16

Table 17. Relay simulation model Feeder 2 without DG.

Relay	Fault current without DG (kA)	Desired PSM	ANN PSM	% difference PSM	Desired TMS	ANN TMS	% difference PSM	Time of operation
R6	3.069	3.491	3.578	0.025	0.52265	0.566	0.083	2.14
R7	2.55	2.760	2.878	0.043	0.51288	0.534	0.0411	2.10
R8	1.527	6.945	6.701	-0.035	0.97867	0.989	0.019	2.08
R9	1.23	6.061	6.123	0.0102	0.89995	0.987	0.098	2.06
R10	1.028	5.578	5.656	0.0140	0.44137	0.566	0.286	1.06
R11	1.003	5.659	5.676	0.003	0.40313	0.467	0.158	0.96
R12	0.958	5.664	5.768	0.018	0.36133	0.397	0.0997	0.86

Table 18. Relay simulation model Feeder 2 with DG.

Relay	Fault current with DG (kA)	Desired PSM	ANN PSM	% difference PSM	Desired TMS	ANN TMS	% difference PSM	Time of operation
R6	5.168	3.49	3.55	0.017	0.522	0.533	0.021	2.14
R7	3.975	2.76	2.87	0.040	0.512	0.520	0.016	2.10

R8	2.431	6.95	6.93	-0.2878	0.979	0.974	-0.5107	2.08
R9	2.061	6.06	6.09	0.4950	0.900	0.906	0.6667	2.06
R10	1.841	5.58	5.60	0.3584	0.441	0.441	0	1.06
R11	1.811	5.66	5.70	0.7067	0.403	0.404	0.2481	0.96
R12	1.756	5.66	5.69	0.5300	0.361	0.364	0.8310	0.86

Table 19. Relay simulation model Feeder 3 without DG.

Relay	Fault current without DG (kA)	Desired PSM	ANN PSM	% difference PSM	Desired TMS	ANN TMS	% difference PSM	Time of operation
R13	0.783	2.61	2.618	0.3065	0.175	0.176	0.5714	0.76
R14	0.722	2.58	2.588	0.3101	0.150	0.151	0.6667	0.66
R15	0.674	2.59	2.605	0.5792	0.128	0.129	0.7813	0.56
R16	0.625	2.60	2.62	0.7692	0.106	0.107	0.9434	0.46
R17	0.538	2.45	2.43	-0.8163	0.077	0.099	1.0204	0.36
R18	0.506	2.530	2.54	0.3953	0.058	0.058	0	0.26

Table 20. Relay Simulation Model Feeder 3 with DG.

Relay	Fault current with DG (kA)	Desired PSM	ANN PSM	% difference PSM	Desired TMS	ANN TMS	% difference PSM	Time of operation
R13	1.614	5.380	5.385	0.0929	0.309	0.311	0.6472	0.76
R14	1.370	4.892	4.894	0.0409	0.253	0.254	0.3953	0.66
R15	1.215	4.673	4.672	-0.0214	0.208	0.210	0.9615	0.56
R16	1.075	4.479	4.480	0.0223	0.166	0.167	0.6024	0.46
R17	0.834	3.790	3.792	0.0528	0.115	0.116	0.8696	0.36
R18	0.763	3.815	3.820	0.1311	0.084	0.085	1.1905	0.26

Table 21. Relay simulation model Feeder 4 without DG.

Relay	Fault current without DG (kA)	Desired PSM	ANN PSM	% difference PSM	Desired TMS	ANN TMS	% difference PSM	Time of operation
R26	2.824	2.076	2.80	0.349	0.385	0.401	0.04	2.20
R27	2.54	1.984	2.01	0.013	0.328	0.330	0.006	2.00
R28	1.758	5.860	5.870	0.1706	0.771	0.785	1.8158	1.80
R29	1.425	5.089	5.090	0.0197	0.630	0.632	0.3175	1.60
R30	1.296	4.984	4.999	0.3010	0.544	0.544	0	1.40
R31	1.062	4.425	4.430	0.1130	0.431	0.432	0.2320	1.20
R32	1.00	4.545	4.546	0.0220	0.366	0.368	0.5464	1.00
R33	0.931	4.655	4.657	0.0430	0.297	0.299	0.6734	0.80

Table 22. Relay simulation model Feeder 4 with DG.

Relay	Fault current with DG (kA)	Desired PSM	ANN PSM	% difference PSM	Desired TMS	ANN TMS	% difference PSM	Time of operation
R26	4.701	3.456	3.460	0.0011	0.657	0.660	0.0046	2.20
R27	4.184	3.268	3.300	0.0098	0.570	0.580	0.018	2.00
R28	2.956	2.463	2.501	0.015	0.389	0.390	0.003	1.80
R29	2.544	9.0857	9.086	0.0033	0.859	0.860	0.1164	1.60
R30	2.376	9.1384	9.146	0.0832	0.754	0.758	0.5305	1.40
R31	1.701	7.0875	7.0956	0.1143	0.570	0.572	0.3509	1.20
R32	1.545	7.0227	7.0546	0.4542	0.473	0.474	0.2114	1.00
R33	1.378	6.8900	6.867	-0.3338	0.374	0.376	0.5348	0.80

Table 23. Relay simulation model Feeder 5 without DG.

Relay	Fault current without DG (kA)	Desired PSM	ANN PSM	% difference PSM	Desired TMS	ANN TMS	% difference PSM	Time of operation
R19	20.647	4.9632	4.509	-0.090	0.852	0.860	0.009	2.20
R20	3.32	3.4583	3.4601	0.0006	0.568	0.603	0.062	1.90
R21	2.635	11.97	11.98	0.0835	0.96	0.965	0.5208	1.60
R22	1.904	9.520	9.601	0.8508	0.71	0.712	0.2817	1.30

Table 24. Relay simulation model Feeder 5 with DG.

Relay	Fault current with DG (kA)	Desired PSM	ANN PSM	% difference PSM	Desired TMS	ANN TMS	% difference PSM	Time of operation
R19	20.908	5.025	5.300	0.055	0.859	0.860	0.0012	2.20
R20	3.327	4.620	4.710	0.019	0.703	0.787	0.119	1.90
R21	2.639	11.996	11.997	0.0083	0.970	0.972	0.2062	1.60
R22	1.906	9.530	9.533	0.0315	0.714	0.716	0.2801	1.30

Table 25. Relay simulation model Feeder 6 without DG.

Relay	Fault current without DG (kA)	Desired PSM	ANN PSM	% difference PSM	Desired TMS	ANN TMS	% difference PSM	Time of operation
R23	6.416	1.6708	1.800	0.078	0.343	0.401	0.169	2.80
R24	3.349	2.4468	2.557	0.045	0.558	0.590	0.058	2.60
R25	2.269	2.8362	2.897	0.022	0.601	0.786	0.308	2.40

Table 26. Relay simulation model Feeder 6 with DG.

Relay	Fault current with DG (kA)	Desired PSM	ANN PSM	% difference PSM	Desired TMS	ANN TMS	% difference PSM	Time of operation
R23	6.861	1.79	1.89	0.056	0.486	0.503	0.035	2.80
R24	3.464	2.56	2.60	0.016	0.786	0.804	0.023	2.60
R25	2.321	3.092	3.80	0.228	0.865	0.876	0.013	2.40

4. CONCLUSION

This study describes the operational analysis of conventional and non-conventional (adaptive) overcurrent relay protection scheme coordination in the presence of DG. The analyses show that the conventional method operates correctly following the sequence of feeder relays calibrations. However, the simulated relay settings have different TMS which varies as the short circuit current changes. If the TMS remains constant, the overcurrent relay will mal-operate and then cause a loss of overcurrent relay coordination of the distribution network protection scheme. The proposed adaptive scheme adjusts the relay setting each time there is a penetration of DG from the remote substation. The RTU constantly monitors the feeder network for in-feed current from the DG and sends any in-feed current to the local station RTU. However, the ANN relay overcurrent model retrains the network each time there is an in-feed current from the remote substation and adjusts its set pattern to the new pattern. The calculated percentage error shows the adaptive nature of the ANN model presented and its accurate operation despite constant adjustment of power system conditions as a result of DG penetration. The proposed scheme shows a more reliable and secure protection.

REFERENCES

[1] Che, L., Khodayar, M.E., Shahidehpour, M., Adaptive protection system for microgrids: Protection practices of a functional microgrid system, IEEE Electrification Magazine, vol. 2, no. 1, 2014, p. 66–80.
[2] Martinez, J.A., Martin-Arnedo, J., Impact of distributed generation on distribution protection and power quality, 2009 IEEE Power Energy Society General Meeting, 2009, p. 1–6.
[3] Manditereza, P.T., Bansal, R., Renewable distributed generation: The hidden challenges – A review from the protection perspective, Renewable Sustainable Energy Reviews, vol. 58, 2016, p. 1457–1465.

[4] Ustun, T.S., Ozansoy, C., Ustun, A., Fault current coefficient and time delay assignment for microgrid protection system with central protection unit, IEEE Transactions on Power Systems, vol. 28, no. 2, 2012, p. 598–606.
[5] Eissa, M.M., Protection techniques with renewable resources and smart grids – A survey, Renewable Sustainable Energy Reviews, vol. 52, 2015, p. 1645–1667.
[6] Conti, S., Analysis of distribution network protection issues in presence of dispersed generation, Electric Power Systems Research, vol. 79, no. 1, 2009, p. 49–56.
[7] Basso, T.S., DeBlasio, R., IEEE 1547 series of standards: Interconnection issues, IEEE Transactions on Power Electronics, vol. 19, no. 5, 2004, p. 1159–1162.
[8] Chen, J., Fan, R., Duan, X., Cao, J., Penetration level optimization for DG considering reliable action of relay protection device constraints, Proceedings of 2009 International Conference on Sustainable Power Generation and Supply, 2009, p. 1–5.
[9] Zhan, H., Wang, C., Wang, Y., Yang, X., Zhang, X., Wu, C., Chen, Y., Relay protection coordination integrated optimal placement and sizing of distributed generation sources in distribution networks, IEEE Transactions on Smart Grid, vol. 7, no. 1, 2015, p. 55–65.
[10] Uthitsunthorn, D., Kulworawanichpong, T., Distance protection of a renewable energy plant in electric power distribution systems, Proceedings of 2010 International Conference on Power System Technology, 2010, p. 1–6.
[11] Zhang, Y., Dougal, R.A., Novel dual-FCL connection for adding distributed generation to a power distribution utility, IEEE Transaction on Applications of Superconductors, vol. 21, no. 3, 2010, p. 2179–2183.
[12] Dehghanpour, E, Karegar, H.K., Kheirollahi, R., Soleymani, T., Optimal coordination of directional overcurrent relays in microgrids by using cuckoo-linear optimization algorithm and fault current limiter, IEEE Transactions on Smart Grid, vol. 9, no. 2, 2016, p. 1365–1375.
[13] Shih, M.Y., Enríquez, A.C., Leonowicz, Z.M., Martirano, L., Mitigating the impact of distributed generation on directional overcurrent relay coordination by adaptive protection scheme, Proceedings of 2016 IEEE 16th international conference on environment and electrical engineering (EEEIC), 2016, p. 1–6.
[14] Shih, M.Y., Conde, A., Leonowicz, Z., Martirano, L., An adaptive overcurrent coordination scheme to improve relay sensitivity and overcome drawbacks due to distributed generation in smart grids, IEEE Transactions on Industrial Applications, vol. 53, no. 6, 2017, p. 5217–5228.
[15] El-Hamrawy, A.H., Ebrahiem, A.A.M., Combined centralized/decentralized communications for power systems equipped with distributed generation, IEEE Access, 2022.
[16] Alipour, A., Pacis, M., Optimal coordination of directional overcurrent relays (DOCR) in a ring distribution network with distributed generation (DG) using genetic algorithm, Proceedings of 2016 IEEE Region 10 Conference (TENCON), 2016, p. 3109–3112.
[17] Yang, H., Wen, F., Ledwich, G., Optimal coordination of overcurrent relays in distribution systems with distributed generators based on differential evolution algorithm, International Transactions on Electrical Energy Systems, vol. 23, no. 1, 2013, p. 1–12.
[18] Alkaran, D.S., Vatani, M.R., Sanjari, M.J., Gharehpetian, G.B., Naderi, M.S., Optimal overcurrent relay coordination in interconnected networks by using fuzzy-based GA method, IEEE Transactions on Smart Grid, vol. 9, no. 4, 2016, p. 3091–3101.
[19] Oudalov, A., Fidigatti, A., Adaptive network protection in microgrids, International Journal of Distributed Energy Resources, vol. 5, no. 3, 2009, p. 201–226.
[20] Ghadiri, S.M.E., Mazlumi, K., Adaptive protection scheme for microgrids based on SOM clustering technique, Applied Soft Computing, vol. 88, 2020, art. no. 106062.
[21] Momesso, A.E., Bernardes, W.M.S., Asada, E.N., Adaptive directional overcurrent protection considering stability constraint, Electric Power Systems Research, vol. 181, 2020, art. no. 106190.
[22] Ram, O.S., Saraswat, A., Goyal, S.K., Sharma, V., Khan, B., Mahela, O.P., Alhelou, H.H., Siano, P., Alienation coefficient and wigner distribution function-based protection scheme for hybrid power system network with renewable energy penetration, Energies, vol. 13, no. 5, 2020, p. 11–20.
[23] Brahma, S.M., Girgis, A.A., Development of adaptive protection scheme for distribution systems with high penetration of distributed generation, IEEE Transactions on Power Delivery, vol. 19, no. 1, 2004, p. 56–63.
[24] Wan, H., Li, K.K., Wong, K.P., An adaptive multi-agent approach to protection relay coordination with distributed generators in industrial power distribution system, IEEE Transactions on Industrial Applications, vol. 46, no. 5, 2010, p. 2118–2124.
[25] Muda, H., Jena, P., Sequence currents based adaptive protection approach for DNs with distributed energy resources, IET Generation, Transmission and Distribution, vol. 11, no. 1, 2017, p. 154–165.
[26] Ustun, T.S., Ozansoy, C., Zayegh, A., Modeling of a centralized microgrid protection system and distributed energy resources according to IEC 61850-7-420, IEEE Transactions Power Systems, vol. 27, no. 3, 2012, p. 1560–1567.

[27] Mahat, P., Chen, Z., Bak-Jensen, B., Bak, C.L., A simple adaptive overcurrent protection of distribution systems with distributed generation, IEEE Transactions on Smart Grid, vol. 2, no. 3, 2011, p. 428–437.
[28] Chakor, V.S., Date, T.N., Optimum coordination of directional overcurrent relay in presence of distributed generation using genetic algorithm, Proceedings of 2016 10th International Conference on Intelligent Systems and Control (ISCO), 2016, p. 1–5.
[29] Swief, R.A., Abdelaziz, A.Y., Nagy, A., Optimail strategy for over current relay coordination using genetic algorithm, Proceedings of 2014 International Conference on Engineering and Technology (ICET), 2014, p. 1–5.
[30] Singh, D.K., Gupta, S., Use of genetic algorithms (GA) for optimal coordination of directional over current relays, Proceedings of 2012 Students Conference on Engineering and Systems, 2012, p. 1–5.
[31] Alam, M.N., Overcurrent protection of AC microgrids using mixed characteristic curves of relays, Computer and Electrical Engineering, vol. 74, 2019, p. 74–88.
[32] Hosseini, S.A., Askarian, A.H., Sadeghi, S.H.H., Razavi, F., Merging the retrieval of the protection coordination of distribution networks equipped with DGs in the process of their siting and sizing, Journal of Renewable and Sustainable Energy, vol. 8, no. 3, 2016, art. no. 035502.
[33] Phadke, A.G., Thorp, J.S., Computer relaying power systems, England: John Wiley and Sons Limited, 2009.
[34] Grossi, E., Buscema, M., Introduction to artificial neural network, European Journal of Gastroenterology and Hepatology, vol. 19, no. 12, 2008, p. 1046–1054.
[35] Akhikpemelo, A., Evbogbal, M., Okundamiya, M., Overcurrent relays coordinations using MATLAB model, Journal of Engineering and Manufacturing Technology, vol. 6, 2018, p. 8–15.
[36] Angaleswari, S., Jamuna, K., Optimal placement and sizing of real power supporting dg in radial distribution network, Proceedings of the 2015 IEEE International Conference on Electrical and Computer Engineering, 2015, p. 342-345.
[37] Okelola, M.O., Olabode, O.E., Ajewole, T.O., Teaching-learning based optimization approach for determining size and location of distributed generation for real power loss reduction on Nigerian grid, UNIOSUN Journal of Engineering and Environmental Sciences, vol. 1, no. 1, 2019, p. 1–10.
[38] Oladepo, O., Ajewole, T.O., Awofolaju, T.T., Optimum utilization of grid-connected hybrid power system using hybrid particle swarm optimization/whale optimization algorithm, Energy Storage, vol. 4, no. 2, 2022, p. 1–14.
[39] Ajewole, T.O., Olawuyi, A.A., Agboola, M.K., Onarinde, O., A comparative study on the performances of power systems load forecasting algorithms, Turkish Journal of Electrical Power and Energy Systems, vol. 1, no. 2, 2021, p. 99–107.
[40] Ajewole, T.O., Oladepo, O., Hassan, K.A., Olawuyi, A.A., Onarinde, O., Comparative analysis of three metaheuristic algorithms in sizing hybrid-source power systems, Turkish Journal of Electrical Power and Energy Systems, vol. 2, no. 2, 2022, p. 1–13.
[41] Venkatesh, B., Ranjan, R., Gooi, H.B., Optimal reconfiguration of radial distribution systems to maximize loadability, IEEE Transactions on Power Systems, vol. 19, no. 1, 2004, p. 260–266.